Article

pubs.acs.org/Biomac

Binary Complex Based on Zein and Propylene Glycol Alginate for Delivery of Quercetagetin

Cuixia Sun, Lei Dai, and Yanxiang Gao*

Beijing Advanced Innovation Center for Food Nutrition and Human Health, Beijing Laboratory for Food Quality and Safety, Beijing Key Laboratory of Functional Food from Plant Resources, College of Food Science & Nutritional Engineering, China Agricultural University, Beijing 100083, China

Supporting Information

ABSTRACT: Propylene glycol alginate (PGA) was found to be able to dissolve in aqueous ethanol solution and applied to interact with zein to form a noncovalent binary complex by the antisolvent coprecipitation method at pH 4.0. Quercetagetin (Q) was employed to explore the Q-delivery potential of Zein-PGA binary complex. A fruit tree-like microstructure was observed for Zein-PGA binary complex as its "branches" were closely adsorbed by zein particles. A solid sponge-like entity was formed after lyophilization of Zein-PGA binary complex colloidal dispersion. A synergistic effect was found between zein and PGA on improving the entrapment efficiency and loading capacity of Q. The incorporation of Q at a high concentration induced a significant effect on the tertiary structure of zein. Electrostatic attraction, hydrogen bond, and hydrophobic effects were mainly involved in the interactions between zein and PGA. Schematics with four possible structures were proposed to explain the formation mechanism of composites.

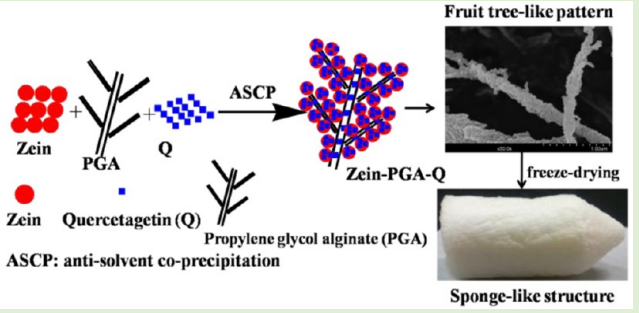

INTRODUCTION

Zein behaves as a prolamin with a molecular weight range from 22 to 40 kDa.[1] Zein consists of more than 50% of nonpolar amino acid residues,[2] and due to its inherent hydrophobicity, zein has been widely studied as a food-grade biopolymer to fabricate particles for encapsulating polyphenols such as quercetin,[3] curcumin,[4] and resveratrol.[5] The combination between proteins and polysaccharides may have improved functional properties compared to the individual polymers.[6,7] For example, composite colloidal particles formed by zein and polysaccharides can provide a better protecting function for nutrients.[8] Previous research focused on using the antisolvent precipitation (ASP) method to prepare composite colloidal particles with a core−shell structure.[9] Specifically, zein was the shell and polysaccharides were coated on its surface to form the outer layer through the electrostatic attraction, and the compound was commonly used as a delivery system for bioactive compounds to improve their stability and bioavailability. However, it is worth mentioning that aforementioned polysaccharides commonly refer to hydrophilic polysaccharides, such as chitosan,[4,8,10,11] pectin,[5,12,13] and gum arabic.[14] Any information on interactions between zein and alcohol-soluble polysaccharides has not been reported due to the fact that polysaccharides are scarcely able to dissolve in aqueous ethanol solution since most of them are prepared by the method of alcohol precipitation.[15] Nevertheless, in our preliminary experiment, propylene glycol alginate (PGA) was found to have a great solubility in aqueous ethanol solution even with a high ethanol concentration (70%, v/v).

PGA is an alginate derivative produced through an esterification reaction between alginic acid and propylene oxide,[16] which is composed of 1,4 linked-D-mannuronic acid (31%−65%) and L-guluronic acid (69%−35%)[17] and is regarded as one distinct group of surface-active food grade polysaccharides ascribed to its propylene glycol groups.[18] Currently, PGA is an approved food additive with attractive properties including viscosity enhancement, stabilization, and film formation.[19,20] The addition of PGA to the alginate suspension imparted emulsifying properties to stabilize the biopolymer blend.[21] Amide bonds could be created between free amine functions of human serum albumin and ester groups of PGA in the inner aqueous phase after alkalization.[22] Nevertheless, PGA is mainly used to improve functional properties of water-soluble proteins. Any investigation into the interactions between PGA and prolamins is not available up to the present.

Quercetagetin (Q), as a characteristic alcohol-soluble flavonol compound, is abundant in *Tagetes* and has a similar structure to quercetin but an additional 6-OH group based on the molecular structure of the flavone backbone (2-phenyl-1,4-benzopyrone). Such a structure with many hydroxyls endows Q with a strong affinity to proteins,[23] and may be able to interact with proteins via noncovalent interactions like hydrophobic effect and hydrogen bonding, which may lead to changes in physicochemical and

Received: September 11, 2016
Revised: November 11, 2016
Published: November 17, 2016

DOI: 10.1021/acs.biomac.6b01362
Biomacromolecules 2016, 17, 3973−3985

functional properties of proteins.[24] Our previous study revealed that Q exhibited stronger antioxidant activity than that of quercetin.[25] In addition, Q has the potential use in the prevention or therapy of cancer and other chronic diseases.[26] However, poor water solubility, low chemical stability, and bioavailability of Q greatly limit its applications. Zein-PGA binary composite colloidal particles were designed as a delivery system for Q in this work to explore its potential application to overcome the above-mentioned disadvantages of Q.

In this study, the method of antisolvent coprecipitation (ASCP) was used to prepare a Q-loaded Zein-PGA binary complex due to the good solubility of individual compounds (zein, PGA, and Q) in aqueous ethanol solution. A hypothesis is proposed that the microstructure and formation mechanism of binary complexes prepared by ASCP may be different from those composites fabricated by ASP, which will be testified by results in the present work. Small-angle X-ray scattering (SAXS) was introduced to explore the interaction among zein, PGA and Q. The effect of Q and PGA on the tertiary structure of zein was initially investigated by near-UV CD, which was scarcely reported in previous studies. Conformational property, and physical, photochemical and thermal stability were also characterized. Findings from this work will provide a theoretical basis for the interaction between alcohol soluble protein and amphiphilic polysaccharide, and may bring a new insight for the development of potential carriers for bioactive compounds.

EXPERIMENTAL SECTION

Materials. Zein with a protein content of 91.3% (w/w) was purchased from Sigma-Aldrich (USA). Absolute ethanol (99.99%), solid sodium hydroxide and liquid hydrochloric acid (36%, w/w) were acquired from Eshowbokoo Biological Technology Co., Ltd. (Beijing, China). Food-grade propylene glycol alginate (PGA) with esterified carboxyl groups of 87.9% was kindly provided by Hanjun sugar industry Co. Ltd. (Shanghai, China). Quercetagetin with the purity of 91% (w/w) was extracted from marigold (*Tageteserecta L.*) flower by the method in our previous study.[21]

Preparation of Q-Loaded Zein-PGA Complex. Q-loaded Zein-PGA complexes were prepared by the antisolvent coprecipitation method adapted from previous study.[27] Briefly, zein (250 mg) and PGA (125 mg) were dissolved in 100 mL of aqueous ethanol solution (70%, v/v) at pH 4.0 adjusted by 0.1 N sodium hydroxide and hydrochloric acid solutions. Different amounts (12.5, 25.0, 50.0, 75.0, and 100.0 mg) of Q powder were added to glass beakers containing Zein-PGA aqueous ethanol solution. The mixtures were bath-sonicated for 20 min, and the resulting Q-loaded Zein-PGA complex suspensions were centrifuged at 765*g* for 10 min to remove the undissolved Q. The final Q-loaded Zein-PGA complex stock solution (40 mL) was injected in 2 min to the beaker containing 120 mL distilled water using a syringe with plunger speed of 20 mL/min.

To acquire aqueous dispersions, approximately three-quarters of ethanol were removed under reduced pressure (−0.1 MPa) by rotary evaporation at 45 °C for 35 min. Finally, Q-loaded Zein-PGA composite colloidal dispersions were adjusted to pH 4.0 using 0.1 N hydrochloric acid solution and stored in the refrigerator at 4 °C for further analysis in the form of liquid, and part of the dispersions were frozen and dried for 48 h with Alpha 1−2 D Plus freeze-drying apparatus (Marin Christ, Germany) to obtain dry particles for solid state characterization analysis. Zein, PGA, Zein-PGA, Zein-Q, and PGA-Q binary complex colloidal dispersions were obtained by the aforementioned process and used as the control sample.

In this work, samples of Q-loaded zein-PGA composite particles with different Q amounts (12.5, 25.0, 50.0, 75.0, and 100.0 mg) were termed as Zein-PGA-Q12.5, Zein-PGA-Q25, Zein-PGA-Q50, Zein-PGA-Q75, and Zein-PGA-Q100, respectively.

Measurement of Particle Size and Zeta-Potential. Particle size and zeta-potential of colloidal dispersions were determined using a combined dynamic light scattering (DLS) and particle electrophoresis instrument (Zetasizer Nano-ZS90, Malvern Instruments Ltd., Worcestershire, UK) according to the descriptions in our previous report.[28] The particle size data reported as cumulative mean diameter (size, nm) was calculated by the intensity weighted using the Stokes−Einstein equation. The zeta-potential of the particles were obtained using the Smoluchowski model through an electrophoretic mobility measurement performed in a capillary electrophoresis device inserted into the DLS instrument. All measurements were carried out at room temperature (25 °C), and each sample was analyzed in triplicate.

Entrapment Efficiency (EE) and Loading Capacity (LC). Freshly prepared colloidal dispersions were centrifuged at 15 000*g* in a refrigerated centrifuge (Sigma, USA) at 25 °C for 30 min. The supernatant was diluted by aqueous ethanol solution (70%, v/v), and the absorption at 358 nm was recorded using a UV-1800 spectrophotometer (Shimadzu Corporation, Kyoto, Japan). The content of Q was quantified against a standard curve of Q dissolved in aqueous ethanol solution (70%, v/v). The EE and LC were calculated by using the following equations:

$$\mathrm{EE}\ (\%) = \frac{\text{total Q} - \text{free Q}}{\text{totalQ}} \times 100$$

$$\mathrm{LC}\ (\%) = \frac{\text{total Q} - \text{free Q}}{\text{total amount of zein and PGA}} \times 100$$

Fluorescence Spectroscopy. Fluorimetric experiments were carried out on a fluorescence spectrophotometer (F-7000, Hitachi, Japan). Scanning parameters were optimized with the slit width of 20 nm for excitation and 10 nm for emission. The excitation wavelength was set at 280 nm to selectively excite the tryptophan residues, and the emission spectra were collected between 290 and 450 nm with a scanning speed of 100 nm/min. Intrinsic fluorescence of protein was measured at a constant concentration of 0.2 mg/mL. All data were collected at room temperature and each individual emission spectrum was the average result of three runs.

Circular Dichroism Spectroscopy. The CD spectra of both far-UV (190−250 nm) and near-UV (250−320 nm) were recorded using a CD spectropolarimeter (Pistar π-180, Applied Photophysics Ltd., Surrey, U.K.). The protein concentration was 0.2 mg/mL, path length was 0.1 and 1.0 cm for far-UV and near-UV region, and constant nitrogen flush was applied during data acquisition. Ellipticity was recorded at a speed of 100 nm/min, 0.2 nm resolution, 20 accumulations, and 2.0 nm bandwidth.

Fourier Transform Infrared Spectroscopy (FTIR). FTIR was used to prove the possible interactions between zein, Q and PGA. Infrared spectra of samples were recorded at room temperature on a Spectrum 100 Fourier transform spectrophotometer (PerkinElmer, UK). Freeze-dried powders were analyzed as KBr pellets according to the description of Lin and Dufresne[29] with some modifications. Briefly, a 2.0 mg sample was mixed with 198.0 mg of pure KBr powder. The mixture was ground into fine powder, pressed into a pellet, and measured by FTIR. The spectra were acquired at the spectral width ranging

DOI: 10.1021/acs.biomac.6b01362
Biomacromolecules 2016, 17, 3973−3985

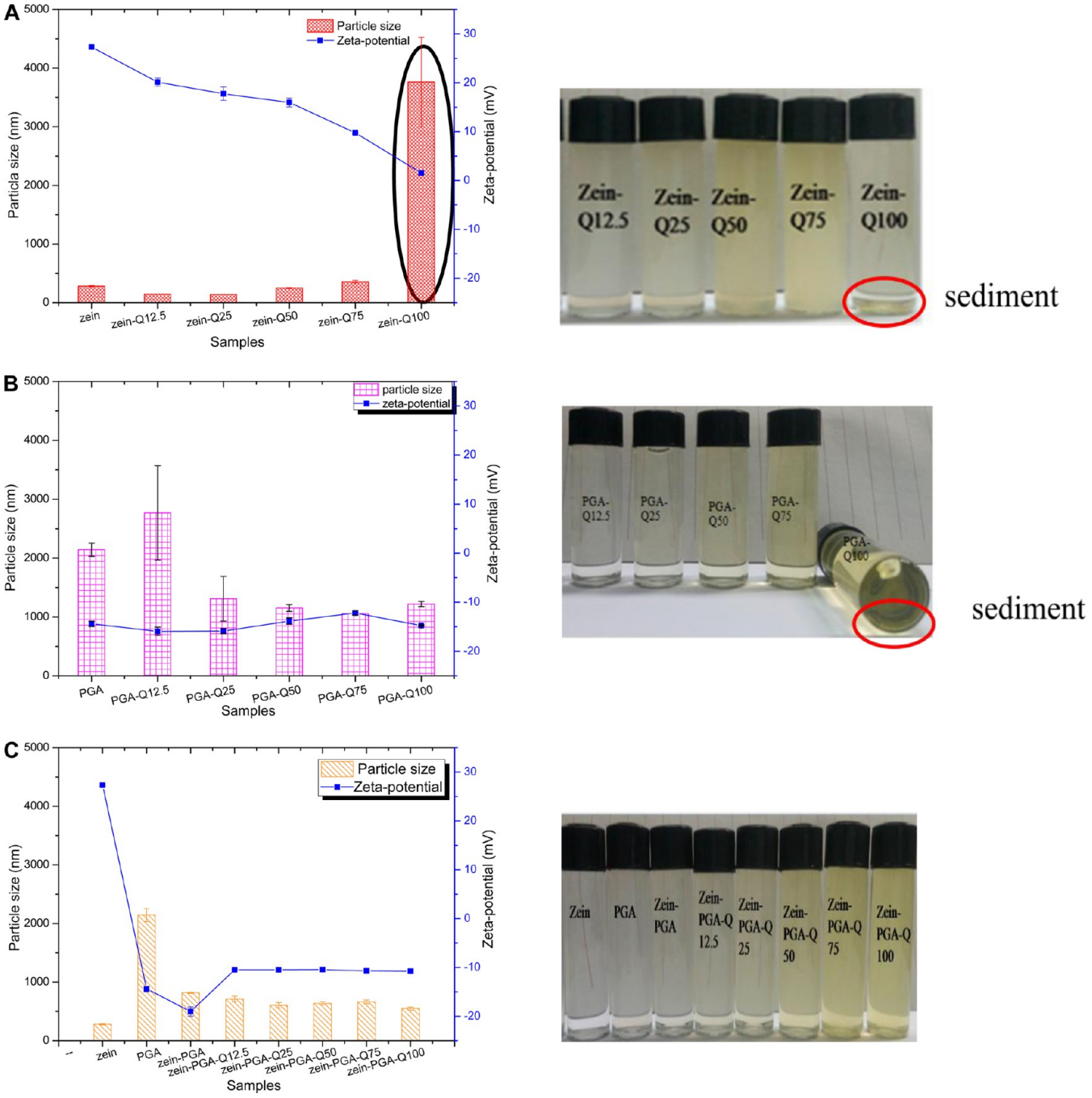

Figure 1. Effect of Q addition at different concentrations on particle size and zeta-potential of colloidal dispersions for Zein (A), PGA (B), and Zein-PGA (C), respectively.

from 4000 to 400 cm^{-1} with a 4 cm^{-1} resolution and an accumulation of 64 scans. Pure KBr powder was used as a baseline.

X-ray Diffraction (XRD). The crystalline structure of the samples was analyzed on a wide-angle X-ray diffractometer (Bruker D8, Germany). The instrument was equipped with a copper anode that produces Cu Kα radiation and was operated at 40 kV of an accelerating voltage and 40 mA of a tube current. The 2θ angle was set from 5° to 50° in continuous mode using a step size of 0.02° and step time of 5 s.

Small-Angle X-ray Scattering (SAXS). SAXS experiments were performed using a SAXSess camera (Anton-Paar, Graz, Austria) to collect information about the structure parameters according to the method of previous study.[30] A PW3830 X-ray generator with a long fine-focus sealed glass X-ray tube (PAN Alytical Almelo, The Netherlands) was operated at 40 kV and 50 mA. A shot exposure period of 900 s was used to acquire the scattering data. The sample-to-detector distance was 261.2 mm and the temperature was kept at 25.0 °C. Data analyses were performed by Guinier methods. $I(q)$ is the scattering intensity and $q = (4\pi/\lambda) \sin(\theta/2)$ is the modulus of the scattering vector with θ the scattering angle and λ the wavelength of the X-ray beam.

Physical Stability. The physical stability of the colloidal dispersions was measured using the LUMiSizer (LUM, Germany) on the base of the determined principle that employs centrifugal sedimentation to accelerate the occurrence of instability

DOI: 10.1021/acs.biomac.6b01362
Biomacromolecules 2016, 17, 3973−3985

phenomena such as sedimentation, flocculation, and creaming.[31] The samples went through centrifugal force, while near-infrared light illuminated the whole sample cell (2 mm of path length) to assess the intensity of transmitted light as a function of time and position over the entire sample length simultaneously. The physical stability was shown as a space- and time-related transmission profile over the sample length. The greater change of the transmission with centrifugation, the worse stability of the colloidal dispersions.[32] The parameters used for the measurement were adapted from Yang et al.[33] as follows: 1.8 mL of colloidal dispersion; rotational speed, 765*g*; performed time, 3600 s; time interval, 30 s; temperature, 25 °C.

Field Emission Scanning Electron Microscopy (FE-SEM). The micromorphology of the lyophilized samples was observed by a field emission scanning electron microscope (FE-SEM, SU8010, Hitachi) at an accelerating voltage of 5.0 kV. Prior to the observation, the surfaces of samples were sputter-coated with a gold layer to avoid charging under the electron beam.

Statistical Analysis. All results are reported as means and standard deviations for at least three replicate samples and statistical differences were evaluated using the SPSS 18.0 for Windows (SPSS Inc., Chicago, USA). Least significant differences ($P < 0.05$) were accepted among the treatments.

RESULTS AND DISCUSSION

Particle Size, Zeta-Potential, EE and LC. The mean particle size and zeta-potential of colloidal dispersions are given in Figure 1. As shown in Figure 1A, the incorporation of Q hardly resulted in the obvious size changes of zein colloidal particles until the highest Q incorporation level (Zein-Q100), which induced a drastic size increase. The result indicated that the excessive Q could not be embedded by the single zein colloidal particles. The increased size may be due to the decreased zeta-potential. It can be observed that zeta-potential of the colloidal dispersions was gradually decreased from +27.3 (zein) to 1.54 mV (Zein-Q100) when the incorporated amount of Q was increased, which reduced the electrostatic repulsion and the phase separation occurred, leading to visible sediments with large sizes at the bottom of the bottle. A similar result was pointed out by Sarika and Nirmala[34] who reported that the presence of curcumin inside gum arabic aldehyde-gelatin nanogel increased the particle size. PGA particles with micro size are shown in Figure 1B, and a large size was found for the sample of PGA-Q12.5, which may be due to the fact that Q inclusion at a low level induced the formation of a relative loose structure between PGA and Q. Continuously increasing the concentration of Q, the particle size was decreased but still in micro scale. Possible explaination was that Q incorporation resulted in the solvatation change of PGA due to the strong interaction between PGA and Q, leading to the formation of PGA-Q complex with more compact structure than that of PGA.

As shown in Figure 1C, the particle size of Zein-PGA binary composite was bigger than that of zein but smaller than that of PGA particles, indicating that the binary complex between zein and PGA was formed at pH 4.0 due to the attractive electrostatic interactions.[35,36] The result was ascribed to the fact that zein and PGA carried opposite charges at pH 4.0, namely, zein contained a net positive charge and PGA had a negative charge since the isoelectric point of zein was 6.2[37] and PGA has a dissociation constant (pK_a) around pH 3.5.[38] An attractive electrostatic interaction between zein and PGA occurred due to the charge neutralization. Zein-PGA binary complex exhibited an overall negative charge, suggesting that the outer layer of the complex was dominated by PGA. Peinado et al.[39] pointed that the outer pectin layer dominated the overall biopolymer particle charge characteristics. The size and zeta-potential of Q-loaded Zein-PGA composite particles had no distinct difference compared to that of Zein-PGA binary complex, indicating that a stable system was formed between zein and PGA.

EE and LC are crucial parameters to evaluate whether the designed encapsulation delivery system is feasible for the potential application. The EE and LC of Q in colloidal dispersions with different formulations are listed in Table 1. As expected, there was a gradual decrease in EE, while an increase of LC with the increase of Q concentration incorporated. All the tested colloidal dispersions with the PGA incorporation showed significantly ($P < 0.05$) higher EE and LC values than that of zein colloidal dispersion. Particularly, for example, the EE of Q in the sample of Zein-PGA-Q50 composite dispersions was 91.7%, and the LC reached to 10.8%. The result may be due to a high molecular weight of 5.6×10^6 Da of PGA, which was 255 fold of zein with 2.2×10^4 Da, resulting in the strong entrapped ability of Q. These findings indicated that zein and PGA showed a synergistic effect on EE and LC of Q. Liang et al.[4] found that N-(2-hydroxyl) propyl-3-trimethylammonium chitosan chloride (HTCC) resulted in a higher EE as the longer chain of the HTCC molecule could entrap more curcumin. These results suggested that Zein-PGA binary complex could be an ideal carrier to be designed delivery system containing the high concentration of functional component.

Table 1. Encapsulation Efficiency (EE) and Loading Capacity (LC) of Q in Colloidal Particles in Different Formulations[a]

samples	EE (%)	LC (%)
Zein-Q12.5	70.9 ± 0.3^{g}	2.0 ± 0.1^{j}
PGA-Q12.5	91.3 ± 0.1^{c}	3.0 ± 0.2^{hi}
Zein-PGA-Q12.5	96.3 ± 0.2^{a}	3.3 ± 0.1^{hi}
Zein-Q25	67.5 ± 0.4^{h}	2.4 ± 0.1^{ij}
PGA-Q25	90.4 ± 0.5^{c}	6.1 ± 0.2^{g}
Zein-PGA-Q25	93.8 ± 0.2^{b}	6.2 ± 0.2^{g}
Zein-Q50	69.9 ± 0.8^{g}	3.1 ± 0.1^{hi}
PGA-Q50	88.1 ± 0.7^{d}	9.3 ± 0.3^{f}
Zein-PGA-Q50	91.7 ± 0.2^{c}	10.8 ± 0.4^{e}
Zein-Q75	63.2 ± 0.6^{i}	3.8 ± 0.1^{h}
PGA-Q75	82.9 ± 0.9^{e}	11.6 ± 0.2^{d}
Zein-PGA-Q75	84.6 ± 0.2^{e}	12.9 ± 0.3^{c}
Zein-Q100	44.1 ± 0.7^{j}	1.1 ± 0.1^{k}
PGA-Q100	79.3 ± 0.2^{f}	14.4 ± 0.5^{b}
Zein-PGA-Q100	84.1 ± 0.3^{e}	15.3 ± 0.4^{a}

[a]Values are means ± SD ($n = 3$). Different superscript letters in the same column indicate significant differences ($P < 0.05$).

Conformational and Structural Properties. The effect of Q incorporation on the fluorescence property of zein is shown in Figure 2A. The fluorescence intensity of zein was gradually decreased upon the increasing concentration of Q, which indicated that the presence of Q resulted in the fluorescence quenching, which may be due to diverse molecular interactions such as molecular rearrangements, energy transfer, ground state complex formation, and collisional quenching.[40] The result in this study was consistent with the report of Joye et al.[9] who found that resveratrol binding to zein resulted in fluorescence quenching of zein. However, a contrast result was obtained from Figure 2 when PGA was added to zein, resulting in the increased fluorescence intensity. The finding may be ascribed to the fact that the formation of Zein−PGA binary complex induced the unfolding

DOI: 10.1021/acs.biomac.6b01362
Biomacromolecules 2016, 17, 3973−3985

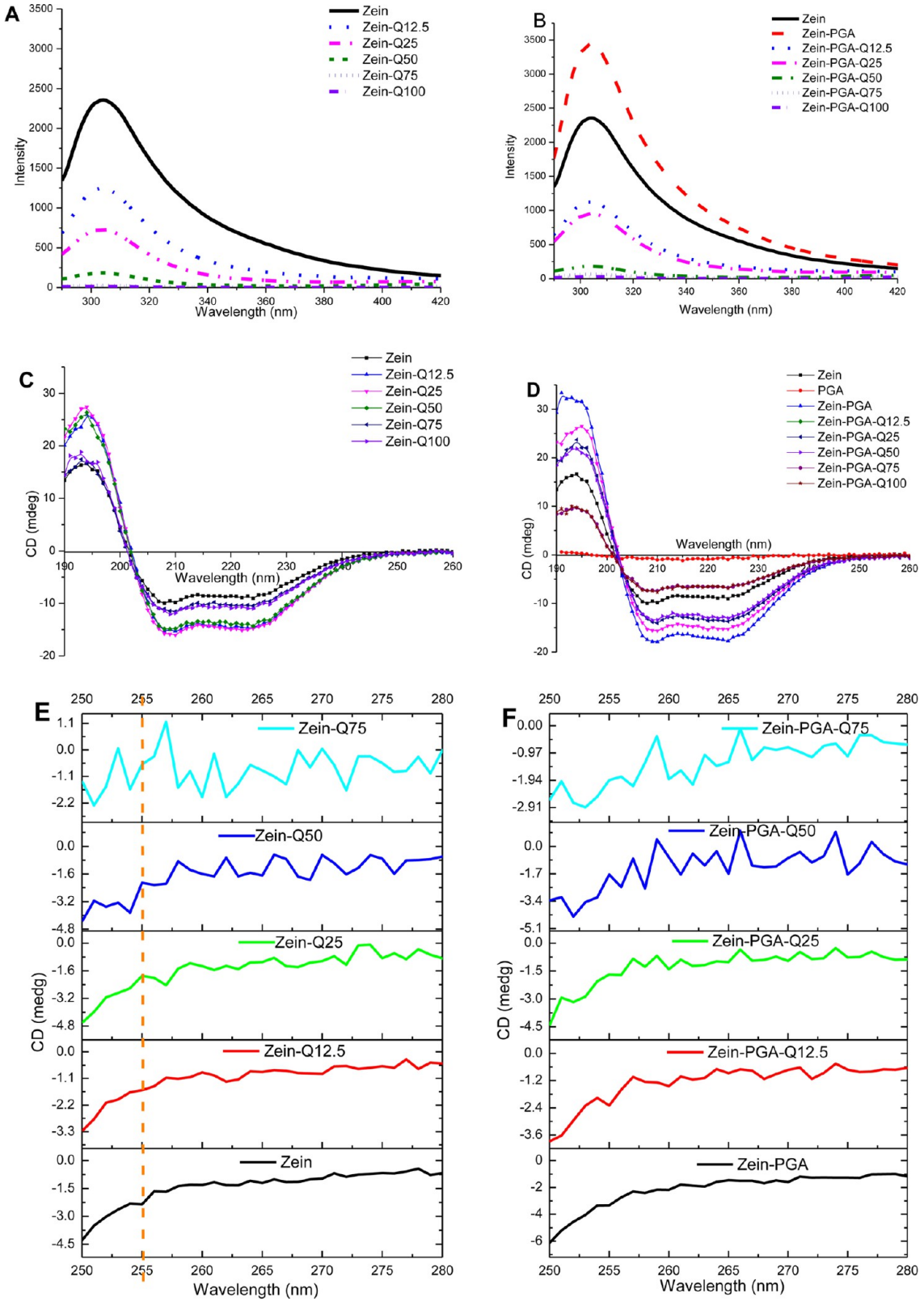

Figure 2. Effects of Q and PGA addition on the fluorescence (A and B), secondary structure (C and D), and tertiary structure (E and F) of zein.

of zein molecule chains, leading to the exposure of tryptophan residues originally located in the hydrophobic interior.[41] In comparison to the complex of Q-loaded zein with the composite of Q-loaded Zein-PGA, the presence of PGA was able to inhibit the fluorescence quenching induced by high Q concentration, for example, the fluorescence intensity of Zein-PGA-Q75 was higher than that of Zein-Q75.

CD was performed to evaluate the secondary structural change of zein. In the CD results as shown in Figure 2C,D, zein showed a positive peak at 193 nm, and two negative peaks at 209 and 223 nm

DOI: 10.1021/acs.biomac.6b01362
Biomacromolecules 2016, 17, 3973−3985

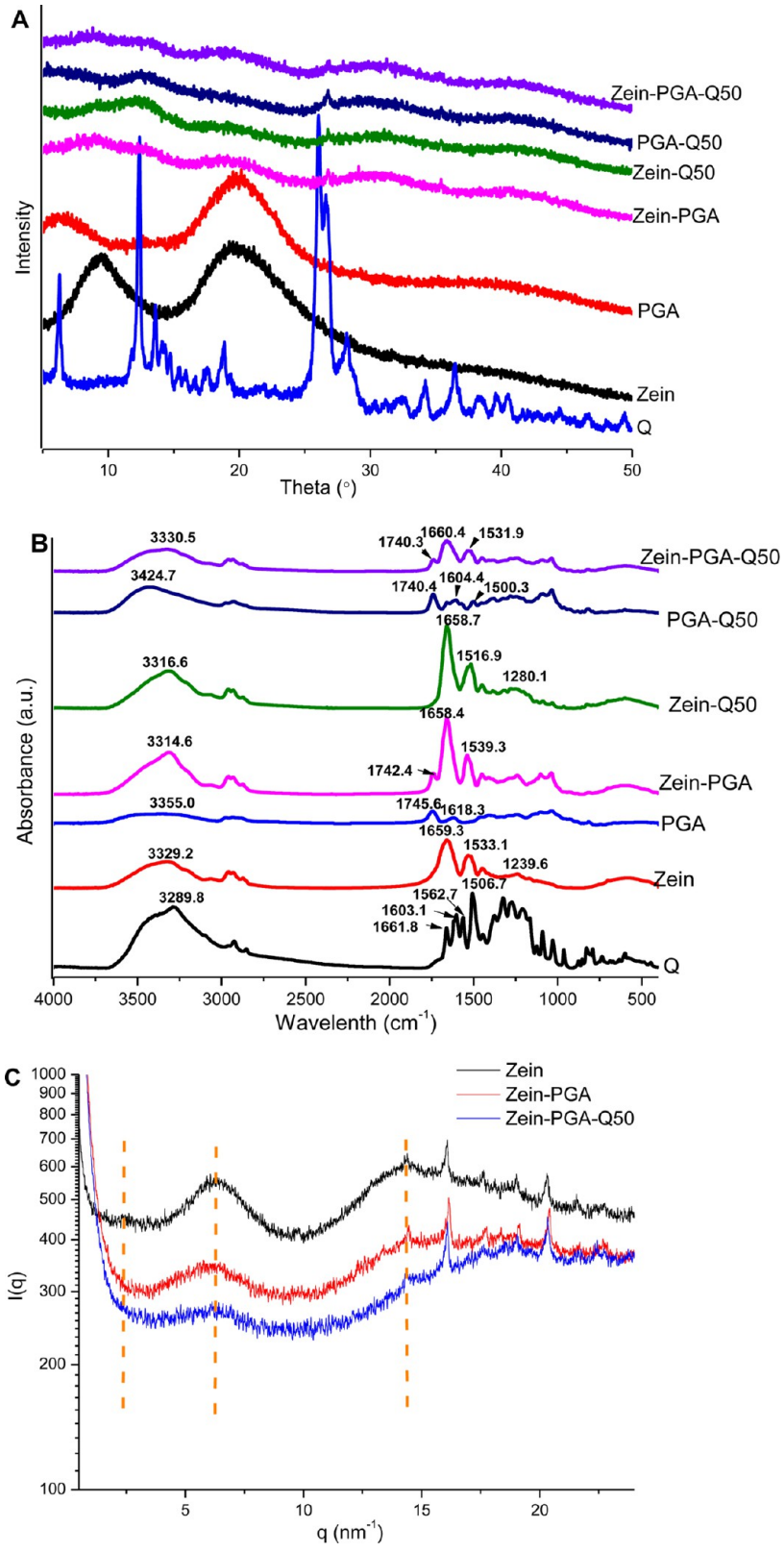

Figure 3. XRD (A), FTIR (B), and SAXS (C) spectra of samples.

with a zero crossing around 202 nm, indicating a characteristic α-helical-rich secondary structure.[42] The presence of both Q and PGA resulted in the increased absolute CD intensities, suggesting the increased content of α-helical structure, which may be due to the conformational relaxation of zein after its interaction with Q or PGA. However, at a high incorporation level of Q in the samples of Zein-PGA-Q75 and Zein-PGA-Q100, decreased absolute CD intensity was observed, revealing that the excessive Q in Zein-PGA binary complex matrix led to the reduced content of α-helical structure consequently accompanied by a great increase

DOI: 10.1021/acs.biomac.6b01362
Biomacromolecules 2016, 17, 3973−3985

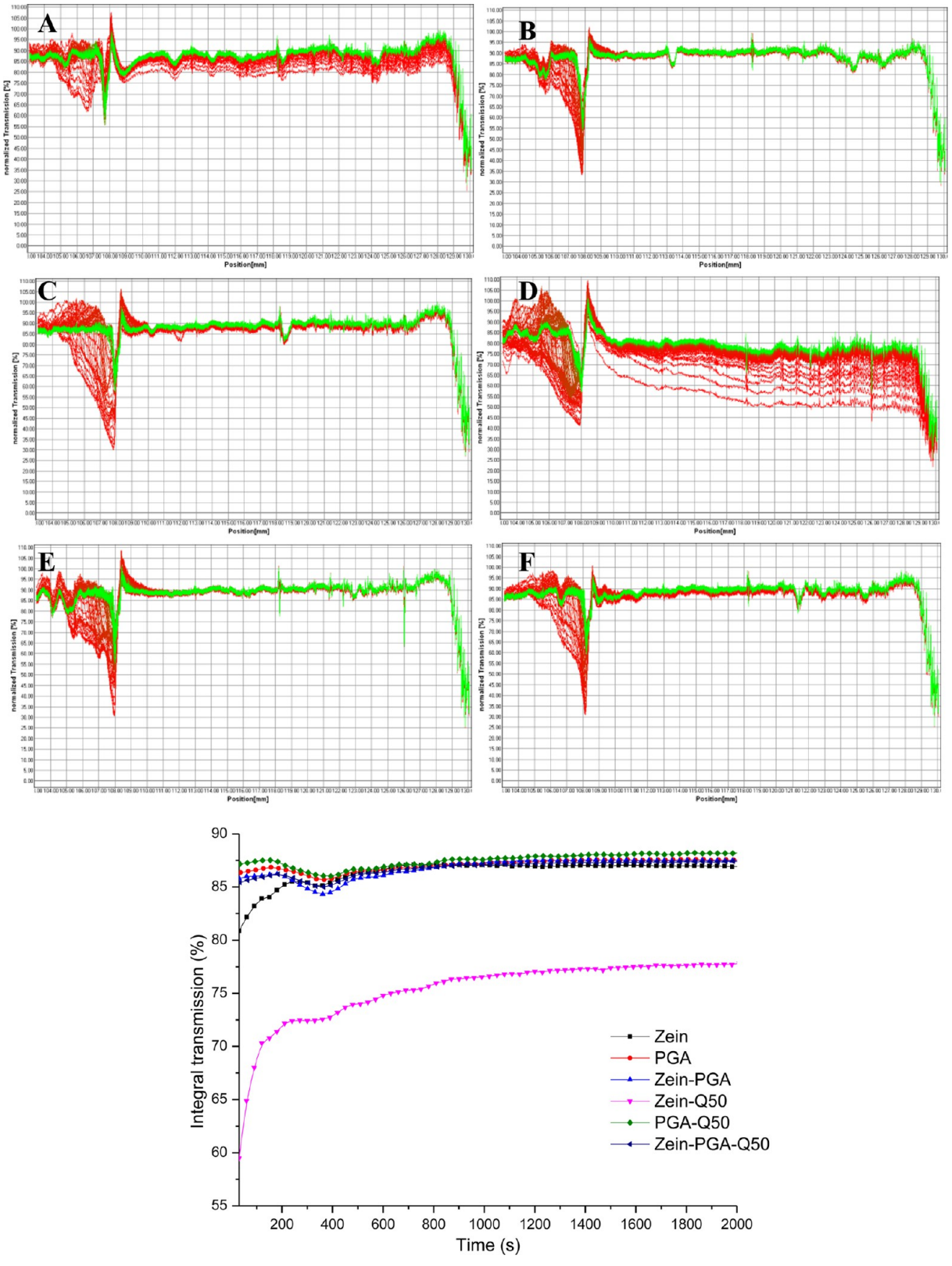

Figure 4. Transmission profiles of Zein (A), PGA (B), Zein-PGA (C), Zein-Q (D), PGA-Q (E), and Zein-PGA-Q (F).

in the amount of β-sheets. The result indicated that the aggregation occurred at a high Q concentration because extended β-sheets were commonly found in aggregated proteins.[43]

Near UV-CD spectra of zein are shown in Figure 2E,F to characterize the effect of Q and PGA incorporation on the tertiary structure of zein. Compared to the spectrum of zein, obvious shift of peak at a wavelength of 255 nm was detected when the high Q concentration was added to zein or Zein-PGA binary complex matrix. The large differences were observed especially relative to high Q concentration in the binary complexes of Zein-Q50 and

DOI: 10.1021/acs.biomac.6b01362
Biomacromolecules 2016, 17, 3973−3985

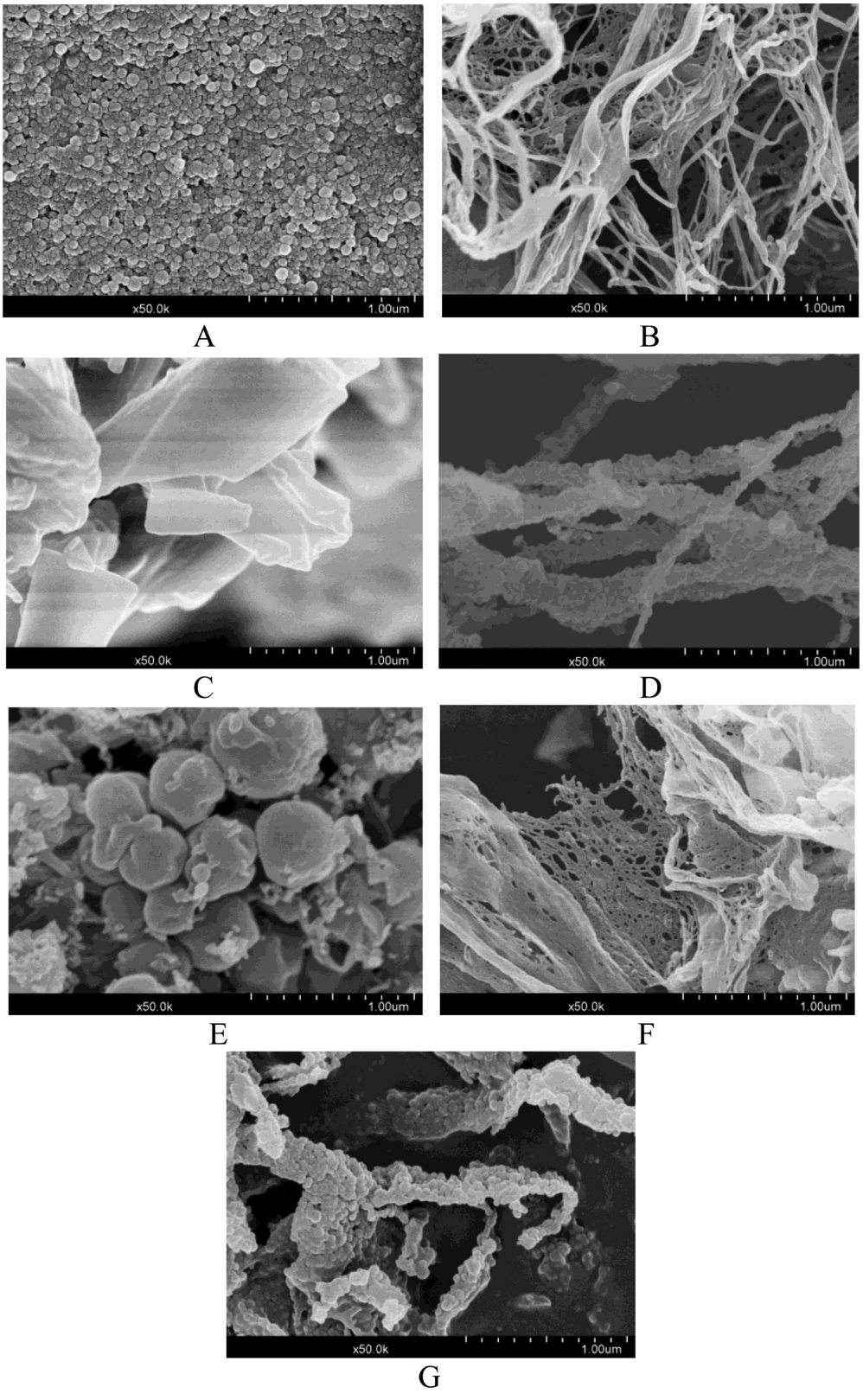

Figure 5. FE-SEM images of Zein (A), PGA (B), Q (C), Zein-PGA (D), Zein-Q (E), PGA-Q (F), and Zein-PGA-Q (G) at a magnification of 50 000×.

Zein-Q75, as well as the composites of Zein-PGA-Q50 and Zein-PGA-Q75, indicating the great change of tertiary structure of zein.[44]

On the basis of the above results, samples of Zein-Q50, PGA-Q50 and Zein-PGA-Q50 complex were selected to be subjected to further study due to the small particle size, relative high EE and LC of Q, and obvious effects on the conformation, secondary and tertiary structure of zein. These samples were termed as Zein-Q, PGA-Q, and Zein-PGA-Q in the following descriptions.

XRD, FTIR, and SAXS. The potential interaction among zein, Q and PGA can be investigated by the shift of peak position and the change of peak intensity for specific bond stretching bands.

DOI: 10.1021/acs.biomac.6b01362
Biomacromolecules 2016, 17, 3973−3985

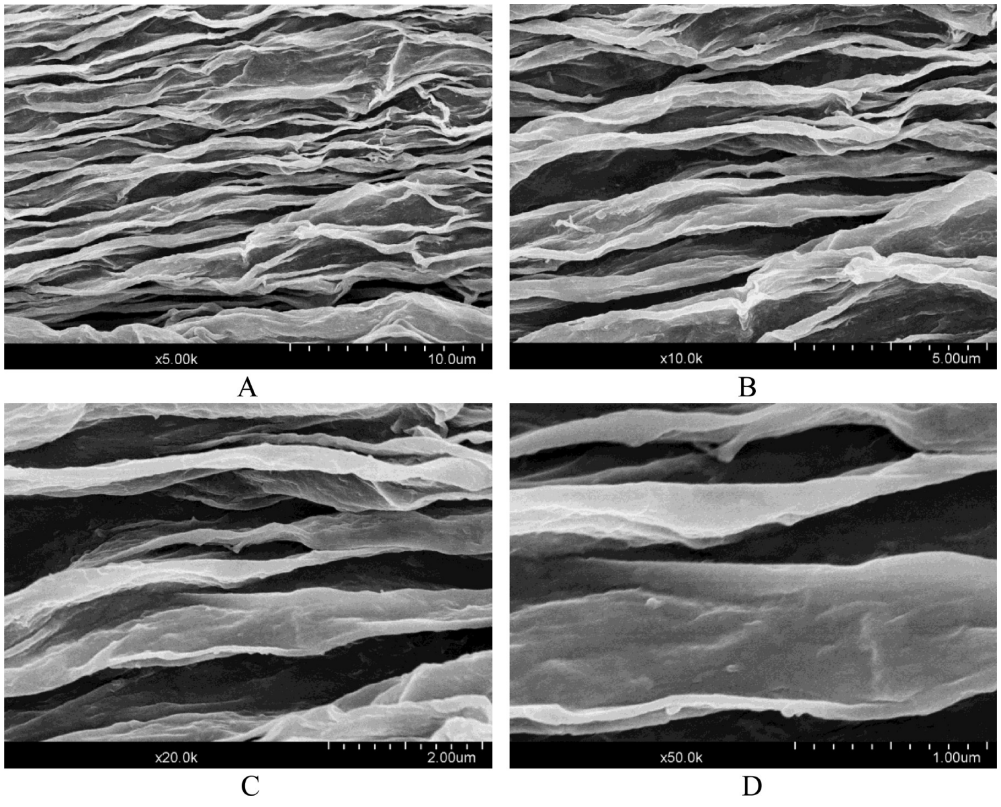

Figure 6. Morphology of PGA alone after thermal treatment at 95 °C for 30 min with different magnifications of 5000× (A), 10 000× (B), 20 000× (C), and 50 000× (D).

Figure 3A shows that zein, Q, and PGA exhibited broad characteristic peaks at 3329.2, 3289.8, and 3355.0 cm^{-1}, respectively. According to the previous report,[45] the band in 3100−3500 cm^{-1} was attributed to hydroxy stretching vibration. The presence of both Q and PGA induced significant shifts of hydrogen bonds to 3316.6, 3314.6, and 3424.7 cm^{-1}, respectively, which implied that strong hydrogen bonds were formed among zein, Q and PGA due to the interaction between amide groups of glutamine in zein and hydroxyl groups in Q and PGA. Similar result has been reported by Luo et al.[46] who found that the hydrogen bonding among zein, carboxymethyl chitosan and vitamin D3 was one of the major forces facilitating nanoparticle formation. Another peak area of 1500−1700 cm^{-1} corresponded to amide I and amide II groups. Amide I (1600−1700 cm^{-1}) was mainly governed by the stretching vibration of C−O and C−N groups,[47] while amid II (1400−1500 cm^{-1}) was due to the bending vibration of N−H groups and stretching vibrations of C−N groups.[48] The bands of amide I and amide II of zein were 1659.3 and 1533.1 cm^{-1}, respectively. When Q or PGA was incorporated, there was no obvious shift of amide I peak for zein, but the intensity was increased, and the bands of amide II groups were obviously shifted to 1516.9 and 1539.3 cm^{-1}, respectively. These findings indicated that other intermolecular forces might exist among zein, Q and PGA, including attractive electrostatic force due to the opposite charges at pH 4.0, and hydrophobic interactions ascribed to the high proportion (more than 50%) of hydrophobic amino acids of zein and the propylene glycol groups of PGA. It was interesting to find that the peaks at 1745.6 cm^{-1} in PGA appeared in the spectra of Zein-PGA binary complexes (1742.4 cm^{-1}) and Q-loaded Zein-PGA composite colloidal particles (1740.3 cm^{-1}). The band of 1800−1650 cm^{-1} was the most significant carbonyl region.[12] New detected peaks suggested that the interaction between carboxyl groups of PGA with amide groups of zein occurred.

Figure 3B shows the crystalline diffraction patterns of samples. Zein and PGA had two flat peaks at diffraction angles 2θ of 9.1° and 19.2°, and 6.9° and 20.2°, respectively, indicating the amorphous nature of the protein and polysaccharide.[49] By contrast, the sharp diffraction peaks of Q suggested its highly crystalline nature. However, XRD diffractograms of complexes for Zein-Q, PGA-Q, and Q-loaded Zein-PGA showed complete loss of the characteristic crystalline peaks of Q. The result suggested that Q was well dispersed in the polymeric matrix and was converted to an amorphous state in the entrapped form possibly mainly due to the intermolecular interactions between Q and PGA within the particle matrix, which thereby provided a persuasive evidence of encapsulation.[3,4,50] Additionally, there was a characteristic new broad peak at the diffraction angle of 30° around appearing on the patterns of the Zein−PGA binary complexes, indicating that the formation of the amorphous complex with intermolecular interaction occurred between zein and PGA. In addition, compared to individual zein and PGA, the peak intensities of Zein-PGA binary complexes at the diffraction angles of both 10° and 20° around were significantly ($P < 0.05$) reduced. These results provided an additional evidence of the noncovalent interaction between zein and PGA, which could be confirmed by the results of FTIR (Figure 3B).

Figure 3C shows the SAXS profiles of zein, Zein-PGA binary complex and Q-loaded Zein-PGA composite. There were three peaks for zein at the scattering modulus (q) of 2.5, 5, and 15 nm^{-1}, respectively. The presence of PGA and Q induced the disappearance of the peak at the scattering modulus of 2.5 nm^{-1}. The scattering intensities of peaks for the samples of Zein-PGA and Zein-PGA-Q composites were greatly reduced, and the

DOI: 10.1021/acs.biomac.6b01362
Biomacromolecules 2016, 17, 3973−3985

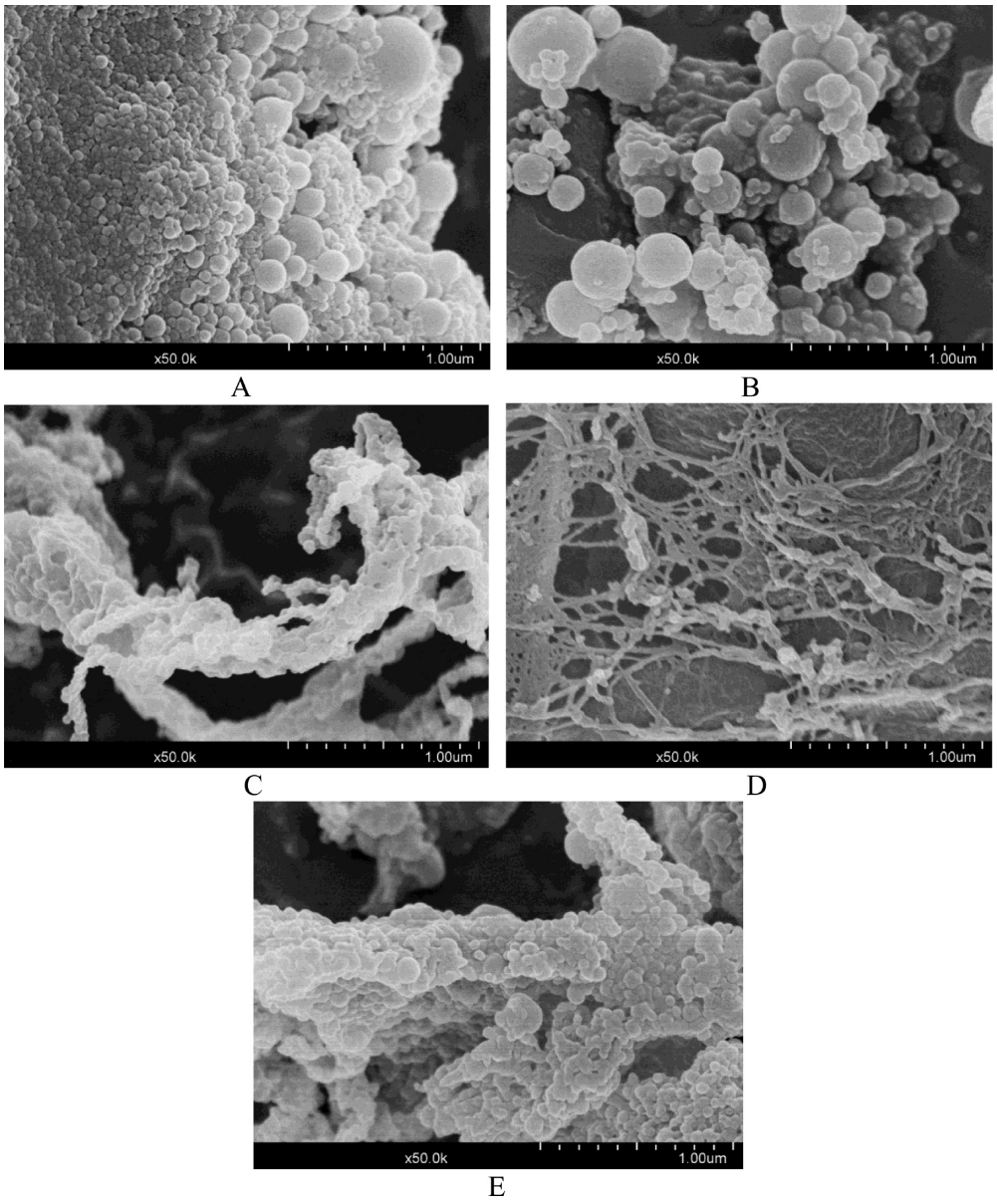

Figure 7. Morphology of freeze-dried samples after thermal treatment at 95 °C for 30 min with a magnification of 50 000×. (A) Zein; (B) Zein-Q; (C) Zein-PGA; (D) PGA-Q; (E) Zein-PGA-Q.

obvious shifting of peaks at the scattering modulus of 5, and 15 nm^{-1} was also observed. The result suggested that the structure of zein was distinctly different from that of Zein-PGA binary complex and Q-loaded Zein-PGA composite. Besides, the curve slopes of binary composites were obviously higher than that of zein, indicating that the particle size became larger after the formation of binary composite colloidal particles.[51,52]

Physical Stability. The stability of colloidal dispersions was expressed as space- and time-related transmission profiles over the sample length (Figure 4), which could be reflected quantitatively by plotting the integrated transmission profiles against the measuring time, and the slope of the resultant curve was inversely related to the stability.[53] The samples of PGA, Zein-PGA, PGA-Q, and Q-loaded Zein-PGA composite exhibited less change in the transmission profiles and low slope values over space and time, indicating better stability of the colloidal dispersions in the presence of PGA than that of Zein-Q binary complex colloidal dispersions. The possible reason was that high Q concentration may be more prone to aggregation and sedimentation in zein colloidal dispersion,[54] while the addition of PGA increased the viscosity of the colloidal dispersions and thus induced more stable dispersions.[55] In addition, first profiles shown in Figure 4 were representative for initial transmission. All the mentioned samples showed higher initial transmission, which further confirmed the improved physical stability of the colloidal dispersions containing PGA because of the change in solvation of PGA due to the intermolecular interaction between PGA and zein or Q.

Micromorphology. The morphological images of samples were captured by FE-SEM with high magnification at 50000× as shown in Figure 5. Zein particles with a uniform size distribution (Figure 5A) were typically spherical as reported in previous study.[56,57] PGA (Figure 5B) exhibited a fine filamentous network structure. Q (Figure 5C) was found to have the morphology of the crystal plate. For the samples of PGA-Q (Figure 5D) and Zein-Q (Figure 5E) binary complexes, Q was inserted in the

DOI: 10.1021/acs.biomac.6b01362
Biomacromolecules 2016, 17, 3973−3985

internal filamentous network structure of PGA, while it was well embedded in zein particles since no free Q was found on the surface of zein particles and the entrapment of Q resulted in larger particles with coarse surface. The formation of Zein-PGA binary complex modified the morphology, which was not spherical or filamentous but a rough branch-like pattern (Figure 5F). Particularly, it can be obviously observed in Figure 5D,G that the surface of "branch" was closely adsorbed by lots of spherical particles. Hadef et al.[58] found that human serum albumin (HSA)-PGA complex microspheres presented a lacework-like structure at lower polymer concentrations. The "branch" seemed to be broken down into relative short thick trunk-like fragments (Figure 5G) when Q was incorporated in the Zein-PGA binary complex matrix, which was still densely covered by zein particles.

The effect of thermal treatment on the morphology of samples was investigated as shown in Figure 6. Figure 6 shows the morphology of PGA alone after thermal treatment at 95 °C for 30 min with different magnifications of 5000× (Figure 6A), 10 000× (Figure 6B), 20 000× (Figure 6C), and 50 000× (Figure 6D). The dense layer-by-layer structures were clearly observed in Figure 6A. With the increase of the magnified multiple, a single piece of wide layer could be seen in Figure 6D, indicating the structural transformation from filamentous network (Figure 6B) to dense layer induced by thermal treatment.

It can been found from Figure 7 that after thermal treatment at 95 °C for 30 min, the spherical structure was retained in zein particles (Figure 7A) but the size was differed, and very large particles were observed. For the sample of Zein-Q complex (Figure 7B), thermal treatment induced the occurrence of the adhesion and even fusion among particles. The more thick branch-like structure was observed in the sample of Zein-PGA binary complex (Figure 7C). The structure of PGA (Figure 6A) went through a transition toward the dense layers, which was converted into a complete compact network for the sample of PGA-Q composite (Figure 7D). However, for the sample of Q-loaded Zein-PGA complex (Figure 7E), the trunk-like fragments seemed to disappear and the bulk aggregates were formed after thermal treatment.

Potential Formation Mechanism. The digital images of the freeze-dried samples are shown in Figure 8A. Native zein existed in powder state with yellow color, which was similar to PGA and Q but with different colors. After the antisolvent coprecipitation process, the sample of Zein-Q complex was still powder but with a fluffy state; however, the presence of PGA induced significant modifications of the existing forms for samples. It can be visually observed that the sample of PGA-Q complex looked like a ball of the soft cotton with long wool, the binary complex of Zein-PGA presented to be a solid sponge-like entity with high density, and the Q-loaded Zein-PGA composite exhibited a medium state between soft cotton and solid sponge-like entity.

According to the cumulative evidence obtained from the various techniques and the visual observation of the lyophilized samples in this work, it can be speculated that four different structures were generated among zein, PGA, and Q after the antisolvent coprecipitation process, and the illustration of the formation mechanism and possible structures are shown in Figure 8B. Q can be embedded inside zein colloidal particles, and the sample of Zein-Q complex kept the original spherical shape, while Q was inserted in the fiber bundle of PGA. Due to attractive electrostatic interaction, hydrogen bond and hydrophobic effects, the binary complex between zein and PGA was formed,

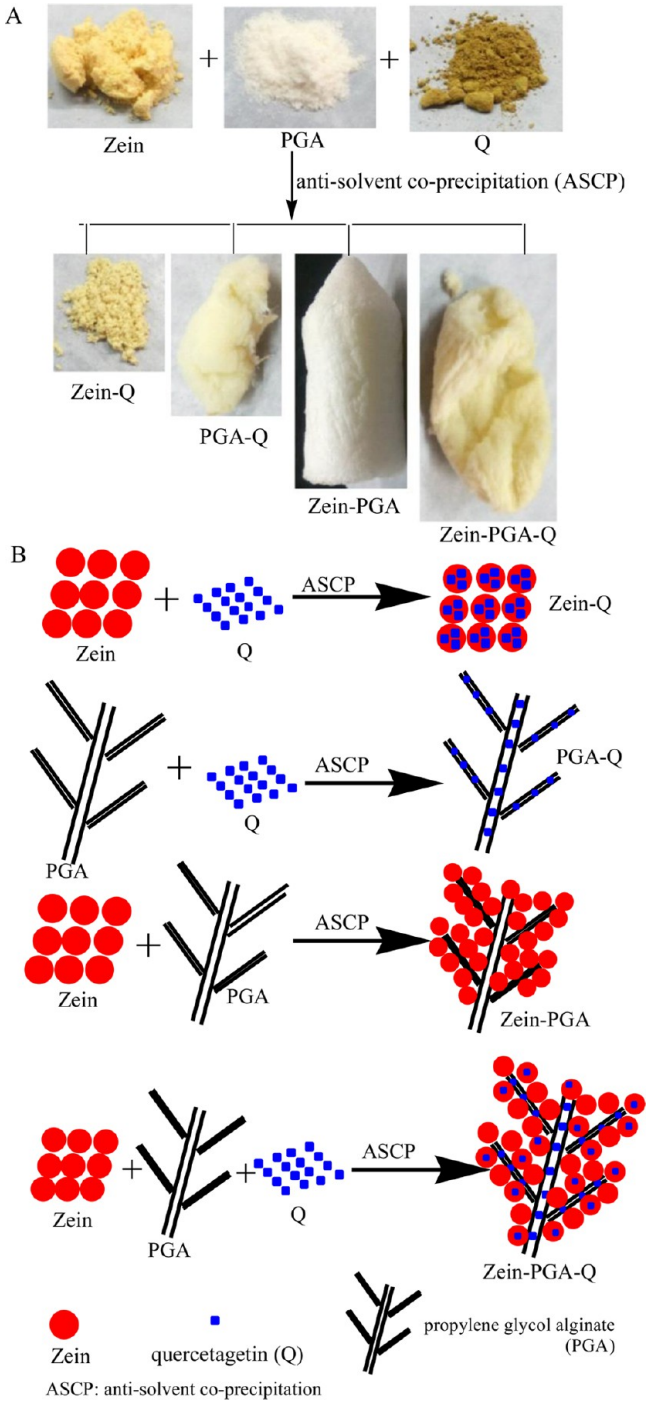

Figure 8. Digital images of the freeze-dried samples (A) and an illustration of the formation mechanism and possible structures of composites (B).

which looked like an apple tree whose branches were full of apples. For the sample of Q-loaded Zein-PGA composite, it can be observed that a tree-like structure was retained, Q was mostly filled in the trunk and branches ascribed to the stronger interaction between PGA and Q than that of zein and Q, a few of Q may be entrapped into zein particles, and zein particles in the presence and absence of Q were closely adsorbed on the branches, indicating that Q-loaded Zein-PGA composite showed the comprehensive features of sphere and filaments, which seemed to be a colorful tree hung with different fruits.

DOI: 10.1021/acs.biomac.6b01362
Biomacromolecules 2016, 17, 3973−3985

CONCLUSIONS

This investigation reported that PGA could completely dissolve in the aqueous ethanol solution (70%, v/v). A solid sponge-like entity was formed between zein and PGA due to noncovalent interactions mainly involved attractive electrostatic force, hydrogen bonding and hydrophobic effects. The tertiary structure of zein was significantly influenced by the addition of Q at the high concentration. The presence of PGA induced characteristic changes of zein, including the increased particle size, enhanced hydrophilicity, and relaxed conformation. Zein-PGA binary complex showed a fruit tree-like structure and the ability to enhance EE and LC of Q. Findings in this work confirmed that Zein-PGA binary complex colloidal particles could be a great delivery system for functional components at a high concentration due to the synergistic effect between zein and PGA, which provided a new idea for the development of potential delivery systems.

ASSOCIATED CONTENT

Supporting Information

The Supporting Information is available free of charge on the ACS Publications website at DOI: 10.1021/acs.biomac.6b01362.

Differential scanning calorimetry thermograms (SI Figure 1); (PDF)

UV irradiation and thermal degradation of Q (SI Figure 2) (PDF)

AUTHOR INFORMATION

Corresponding Author

*E-mail: gyxcau@126.com.

ORCID

Yanxiang Gao: 0000-0003-2331-5956

Notes

The authors declare no competing financial interest.

ACKNOWLEDGMENTS

Financial support from the National Natural Science Foundation of China (No. 31371835) is gratefully acknowledged.

REFERENCES

(1) Torres-Giner, S.; Gimenez, E.; Lagarón, J. M. *Food Hydrocolloids* **2008**, *22*, 601−614.
(2) Lawton, J. W. *Cereal Chem.* **2002**, *79*, 1−18.
(3) Patel, A.; Hu, Y.; Tiwari, J. K.; Velikov, K. P. *Soft Matter* **2010**, *6*, 6192−6199.
(4) Liang, H. S.; Zhou, B.; He, L.; An, Y. P.; Lin, L. F.; Li, Y.; Liu, S. H.; Chen, Y. J.; Li, B. *RSC Adv.* **2015**, *5*, 13891−13900.
(5) Davidov-Pardo, G.; Joye, I. J.; McClements, D. J. *Food Hydrocolloids* **2015**, *45*, 309−316.
(6) Dickinson, E. *Trends Food Sci. Technol.* **1998**, *9*, 347−354.
(7) Schmitt, C.; Turgeon, S. L. *Adv. Colloid Interface Sci.* **2011**, *167*, 63−70.
(8) Luo, Y.; Zhang, B.; Whent, M.; Yu, L. L.; Wang, Q. *Colloids Surf., B* **2011**, *85*, 145−152.
(9) Joye, I. J.; Davidov-Pardo, G.; Ludescher, R. D.; McClements, D. J. *Food Chem.* **2015**, *185*, 261−267.
(10) Park, C. E.; Park, D. J.; Kim, B. K. *Food Sci. Biotechnol.* **2015**, *24*, 1725−1733.
(11) Wang, L. J.; Hu, Y. Q.; Yin, S. W.; Yang, X. Q.; Lai, F. R.; Wang, S. Q. *J. Agric. Food Chem.* **2015**, *63*, 2514−2524.
(12) Hu, K.; Huang, X.; Gao, Y.; Huang, X.; Xiao, H.; McClements, D. J. *Food Chem.* **2015**, *182*, 275−281.
(13) Soltani, S.; Madadlou, A. *Food Hydrocolloids* **2015**, *43*, 664−669.
(14) Chen, H.; Zhong, Q. *Food Hydrocolloids* **2015**, *43*, 593−602.
(15) Kulkarni, S. G.; Vijayanand, P. *LWT-Food Sci. Technol.* **2010**, *43*, 1026−1031.
(16) BeMiller, J. N.; Huber, K. C. *Fennema's Food Chemistry*; CRC Press: Boca Raton, FL, 2008.
(17) Sarker, D. K.; Wilde, P. J. *Colloids Surf., B* **1999**, *15*, 203−213.
(18) Baeza, R.; Pilosof, A. M. R.; Sanchez, C. C.; Rodríguez Patino, J. M. *AIChE J.* **2006**, *52*, 2627−2638.
(19) Hambleton, A.; Debeaufort, F.; Bonnotte, A.; Voilley, A. *Food Hydrocolloids* **2009**, *23*, 2116−2124.
(20) Fabra, M. J.; Talens, P.; Chiralt, A. *Carbohydr. Polym.* **2008**, *74*, 419−426.
(21) Pettitt, D. J.; Wayne, J. E. B.; Nantz, J. J. R.; Shoemaker, C. F. *J. Food Sci.* **1995**, *60*, 528−531.
(22) Hadef, I.; Rogé, B.; Edwards-Lévy, F. *Biomacromolecules* **2015**, *16*, 2296−2307.
(23) Cotin, S.; Calliste, C. A.; Mazeron, M. C.; Hantz, S.; Duroux, J. L.; Rawlinson, W. D.; Ploy, M.-C.; Alain, S. *Antiviral Res.* **2012**, *96*, 181−186.
(24) Labuckas, D. O.; Maestri, D. M.; Perello, M.; Martínez, M. L.; Lamarque, A. L. *Food Chem.* **2008**, *107*, 607−612.
(25) Gong, Y.; Hou, Z.; Gao, Y.; Xue, Y.; Liu, X.; Liu, G. *Food Bioprod. Process.* **2012**, *90*, 9−16.
(26) Baek, S.; Kang, N. J.; Popowicz, G. M.; Arciniega, M.; Jung, S. K.; Byun, S.; Lee, K. W.; et al. *J. Mol. Biol.* **2013**, *425*, 411−423.
(27) Zhong, Q.; Jin, M. *Food Hydrocolloids* **2009**, *23*, 2380−2387.
(28) Sun, C.; Dai, L.; He, X.; Liu, F.; Yuan, F.; Gao, Y. *Food Hydrocolloids* **2016**, *58*, 11−19.
(29) Lin, N.; Dufresne, A. *Biomacromolecules* **2013**, *14*, 871−880.
(30) Zou, Y.; Guo, J.; Yin, S. W.; Wang, J. M.; Yang, X. Q. *J. Agric. Food Chem.* **2015**, *63*, 7405−7414.
(31) Sobisch, T.; Lerche, D. *Colloids Surf., A* **2008**, *331*, 114−118.
(32) Yuan, F.; Xu, D.; Qi, X.; Zhao, J.; Gao, Y. *Food Bioprocess Technol.* **2013**, *6*, 1024−1031.
(33) Yang, W.; Xu, C.; Liu, F.; Sun, C.; Yuan, F.; Gao, Y. *J. Agric. Food Chem.* **2015**, *63*, 5046−5054.
(34) Sarika, P. R.; Nirmala, R. J. *Mater. Sci. Eng., C* **2016**, *65*, 331−337.
(35) Chen, B.; Li, H.; Ding, Y.; Suo, H. *LWT-Food Sci. Technol.* **2012**, *47*, 31−38.
(36) Bengoechea, C.; Jones, O. G.; Guerrero, A.; McClements, D. J. *Food Hydrocolloids* **2011**, *25*, 1227−1232.
(37) Shukla, R.; Cheryan, M. *Ind. Crops Prod.* **2001**, *13*, 171−192.
(38) Harnsilawat, T.; Pongsawatmanit, R.; McClements, D. J. *Food Hydrocolloids* **2006**, *20*, 577−585.
(39) Peinado, I.; Lesmes, U.; Andres, A.; McClements, J. D. *Langmuir* **2010**, *26*, 9827−9834.
(40) Lakowicz, J. R.; Masters, B. R. *J. Biomed. Opt.* **2008**, *13*, 029901.
(41) Peinado, I.; Lesmes, U.; Andres, A.; McClements, J. D. *Langmuir* **2010**, *26*, 9827−9834.
(42) Cabra, V.; Arreguin, R.; Vazquez-Duhalt, R.; Farres, A. *Biochim. Biophys. Acta, Proteins Proteomics* **2006**, *1764*, 1110−1118.
(43) Lefevre, T.; Subirade, M. *Biopolymers* **2000**, *54*, 578−586.
(44) Selling, G. W.; Hamaker, S. A.; Sessa, D. J. *Cereal Chem.* **2007**, *84*, 265−270.
(45) Cerqueira, M. A.; Souza, B. W. S.; Teixeira, J. A.; Vicente, A. A. *Food Hydrocolloids* **2012**, *27*, 175−184.
(46) Luo, Y.; Teng, Z.; Wang, Q. *J. Agric. Food Chem.* **2012**, *60*, 836−843.
(47) Pereira, R. N.; Souza, B. W.; Cerqueira, M. A.; Teixeira, J. A.; Vicente, A. A. *Biomacromolecules* **2010**, *11*, 2912−2918.
(48) Hoque, M. S.; Benjakul, S.; Prodpran, T. *Food Hydrocolloids* **2011**, *25*, 82−90.
(49) Luo, Y.; Wang, T. T.; Teng, Z.; Chen, P.; Sun, J.; Wang, Q. *Food Chem.* **2013**, *139*, 224−230.
(50) Shaikh, J.; Ankola, D. D.; Beniwal, V.; Singh, D.; Kumar, M. R. *Eur. J. Pharm. Sci.* **2009**, *37*, 223−230.
(51) Zou, Y.; Guo, J.; Yin, S. W.; Wang, J. M.; Yang, X. Q. *J. Agric. Food Chem.* **2015**, *63*, 7405−7414.
(52) Iwasaki, Y.; Takemoto, K.; Tanaka, S.; Taniguchi, I. *Biomacromolecules* **2016**, *17*, 2466−2471.

DOI: 10.1021/acs.biomac.6b01362
Biomacromolecules 2016, 17, 3973−3985

(53) Petzold, G.; Goltzsche, C.; Mende, M.; Schwarz, S.; Jaeger, W. *J. Appl. Polym. Sci.* **2009**, *114*, 696−704.
(54) Liu, Y. J.; Liu, D. D.; Zhu, L.; Gan, Q.; Le, X. Y. *Food Res. Int.* **2015**, *74*, 97−105.
(55) Zhang, W.; Xu, F. *ACS Sustainable Chem. Eng.* **2015**, *3*, 2694−2703.
(56) Subramanian, S.; Sampath, S. *Biomacromolecules* **2007**, *8*, 2120−2128.
(57) Liu, F.; Ma, C.; McClements, D. J.; Gao, Y. *Food Hydrocolloids* **2017**, *63*, 625−634.
(58) Hadef, I.; Rogé, B.; Edwards-Lévy, F. *Biomacromolecules* **2015**, *16*, 2296−2307.

DOI: 10.1021/acs.biomac.6b01362
Biomacromolecules 2016, 17, 3973−3985